Communication in Physical Sciences, 2024, 11(3): 509-523

Formation Evaluation Using Integrated Petrophysical Data Analysis of Maboro Field Niger Delta Sedimentary Basin, Nigeria

Ajogwu Cordelia Odinaka*, Aaron Auduson, Tope Alege and Yusuf Odunsanwo

Received: 02 April 2024/Accepted 13 June 2024/Published :16 June 2024

Abstract : T*his study investigates the petrophysical characteristics of the Maboro-Field sand reservoir in the Niger Delta Basin to understand the reasons for its poor hydrocarbon production. Hydrocarbon exploration remains crucial due to the significance of hydrocarbons as primary energy sources. Formation evaluation, encompassing lithology identification, well-log correlation, and petrophysical parameter estimation, was employed to assess the reservoir quality. The analysis involved gamma ray, resistivity, neutron, and density logs from three wells, coupled with 3-D seismic data interpretation using the variance attribute method. The study identified four primary lithologies: sandstone, shale-rich sandstone, sand-rich shale, and shale. Porosity, water saturation, and net pay thickness were evaluated, revealing that CO-01 and CO-03 wells have zones with commercial quantities of hydrocarbons, while CO-02 showed limited potential. Variations in gamma ray signatures indicated lateral continuity of the sand reservoirs, with thirteen hydrocarbon-bearing sands delineated. The 3-D seismic data indicated favorable structural deposition for hydrocarbon accumulation. The findings highlight the varying quality of the reservoirs, with some zones showing high porosity and hydrocarbon saturation, while others were affected by high shale volume and poor porosity. The volumetric analysis estimated the stock tank oil initially in place (STOOIP) and gas initially in place (GIIP), indicating significant gas reserves in several reservoirs. The study demonstrates that petrophysical analysis, integrating well log data and seismic interpretation, effectively identifies productive zones and provides insights into the reservoir's potential for hydrocarbon production.*

Keywords: *Hydrocarbon; Petrophysics; reservoir; seismic***.**

Ajogwu Cordelia Odinaka*
Department of Geology, Federal University, Lokoja, Kogi State, Nigeria
Email: cordeliaajogwu@gmail.com
Orcid: 0009-0000-5489-3893

Aaron Auduson
Department of Geology, Federal University, Lokoja, Kogi State, Nigeria
Email: Aaron.auduson@fulokoja.edu.ng

Tope Alege
Department of Geology, Federal University, Lokoja, Kogi State, Nigeria
Email: Tope.alege@fulokoja.edu.ng

Yusuf Odunsanwo
Dhammatan Oil Nigeria Limited Lagos, Lagos State, Nigeria
Email: sanwo_lanre@yahoo.com

1.0 Introduction

The quest for hydrocarbon exploration is of utmost importance in petrology, as hydrocarbons, including crude oil, natural gas, and coal, serve as the primary sources of energy (Yergin, 1992). Petroleum geologists aim to understand the distribution, quantity, and quality of hydrocarbons within a particular basin before drilling (Press & Raymond, 2003). Formation evaluation, a critical analytical process, plays a key role in identifying economically productive hydrocarbon reservoirs and estimating hydrocarbon volumes within specific zones (Alege *et al*., 2020a).

Formation evaluation involves studying the characteristics of rocks and their relationship to the fluids they contain, both in static and flowing states. Conventional methods focus on analyzing and interpreting petrophysical (well log) data to determine the physical properties (porosity, permeability, water saturation) of hydrocarbon-bearing rocks (Auduson, 2018). Borehole geophysics, concerned with recording and analyzing measurements of physical properties in boreholes, provides valuable insights into subsurface formations.

Despite advances in formation evaluation techniques, there are still challenges, particularly in understanding and optimizing hydrocarbon production in specific reservoirs. In the Maboro Field of the Niger Delta Sedimentary Basin, Nigeria, there is observed poor hydrocarbon production from the sand reservoirs, indicating a knowledge gap in reservoir characterization and productivity. Therefore, there is a need to investigate the underlying reasons for this poor production. The goal of this study is to conduct an integrated petrophysical data analysis of the Maboro Field to understand the factors contributing to the poor hydrocarbon production in the sand reservoirs. By examining the petrophysical characteristics of the reservoir rocks, including porosity, water saturation, and other parameters, from both well log and seismic data, this study aims to identify potential reservoir challenges and opportunities for optimization.

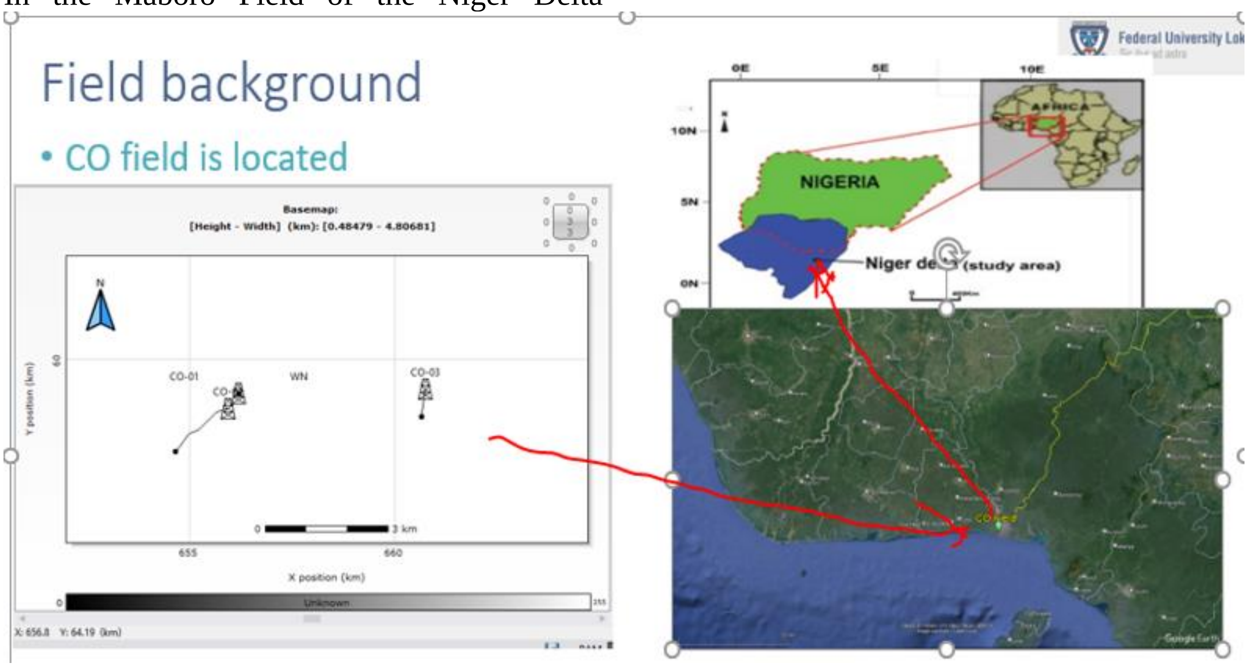

Fig.1: Map of Nigeria and Base map of the studied Area Latitude: 4.5^{o}N to 5.5^{o}N Longitude: 6.5^{o}E to 7.5^{o}E. (modified after Corredor *et al*., 2005)

1.1 Geology of the studied area

Maboro-field is located offshore depositional belt, Eastern Niger Delta Basin; the Niger Delta Basin is situated in the Gulf of Guinea on the West Coast of Central Africa (*Fig.* 1). The Delta built out into the Atlantic Ocean at the mouth of the Niger-Benue River system during the Tertiary (Reijers, 2011). Accumulation of marine sediments in the basin probably commenced in Albian time (199Ma-112Ma), after the opening of the South Atlantic Ocean during the break-up of the African and American continents.

This field was discovered by the drilling of CO-1 well in 1997. The well was drilled to test for hydrocarbons trapped in the sandstones of the Miocene Agbada Formation. The well was planned to penetrate an elongate, east-west trending 4-way dip closed structure at the top of the Agbada Formation level (Dhammatan, 1997). Three wells have been drilled to date. The stratigraphic column (*Fig.* 2) is composed of Paleocene to Pliocene marine shales1 of the Akata Formation that are overlain by the prospective pro-delta, delta channel and beach sands (with intercalated shales) of the Eocene to Recent Agbada Formation (Nton *et al*., 2011). The massive Eocene overlies this "paralic" sequence to the Pleistocene Benin Formation with continental fresh-water bearing sands.

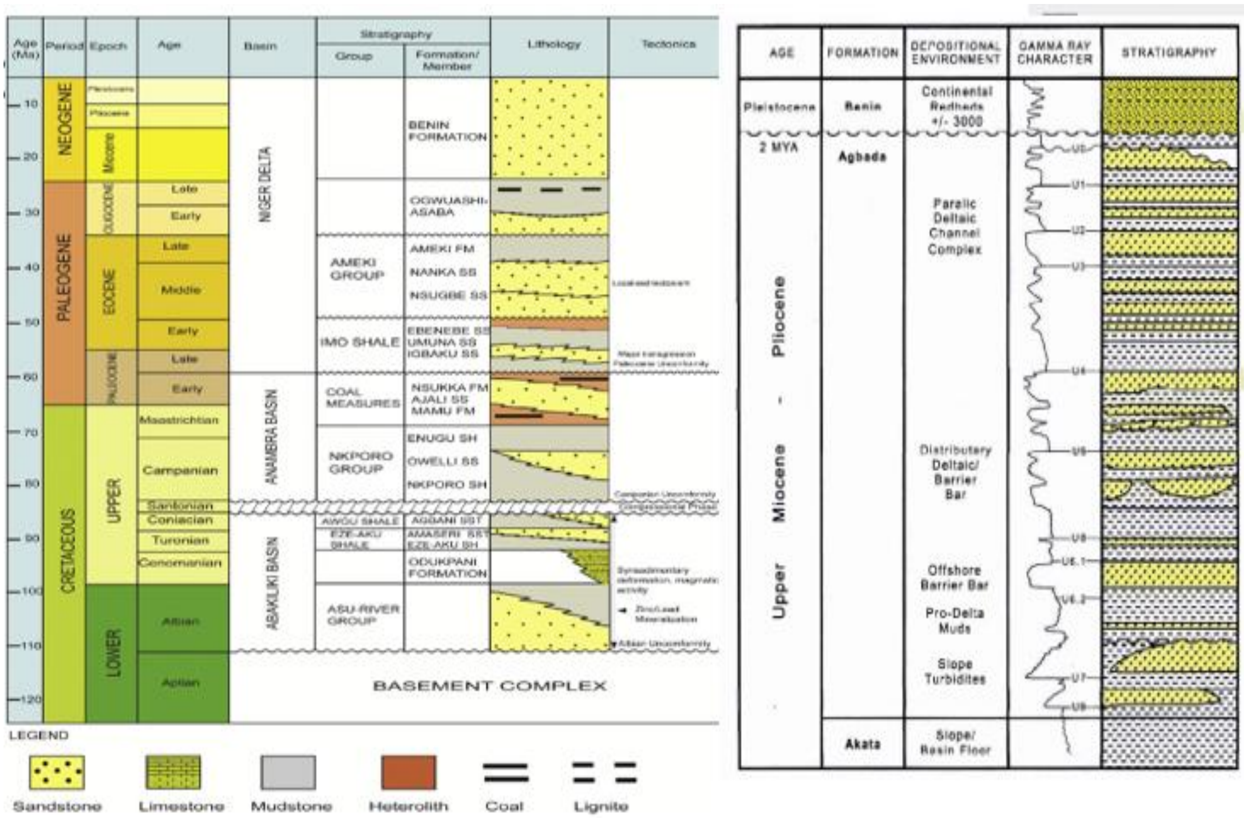

Fig. 2: Stratigraphic successions in the Lower Benue Trough, Niger Delta stratigraphic column around Moboro-field (after Short & Stauble, 1967; Nwajide *et al*., 2005)

2.0 Materials and Methods

2.1 Materials

The materials used for this study include well data (Las files) for three wells from a multinational Oil company, and the study area is covered by 99.9 Km2 of 3-D seismic in SEG-Y format (*Fig.* 6). The quality of the three-dimensional seismic data is fair to good with continuous reflections and well-imaged faults. Overall, data is adjudged to be fair for the interpretation.

The available data and well logs with their depth of penetration (Table 1), respectively. All the wells have the basic log suite. For this study, Schlumberger's Petrel and Techlog software was used for all the interpretations.

Table 1: Available log suite at depths

well	Gamma ray log Top-depth(FT/MD)	Resistivity log top-depth(FT/MD)	Neutron log Top-depth(FT/MD)	Density log Top-bot(FT/MD)	Sonic log
CO-01	0 – 6150	907 -6150	2482 -6150	2482 -6150	NA
CO-02	2504 -11195	2504 - 11195	2504 -11150	2504- 11150	NA
CO-03	2250 – 8068	2250 - 8068	2250 – 8068	8068 – 2250	8068

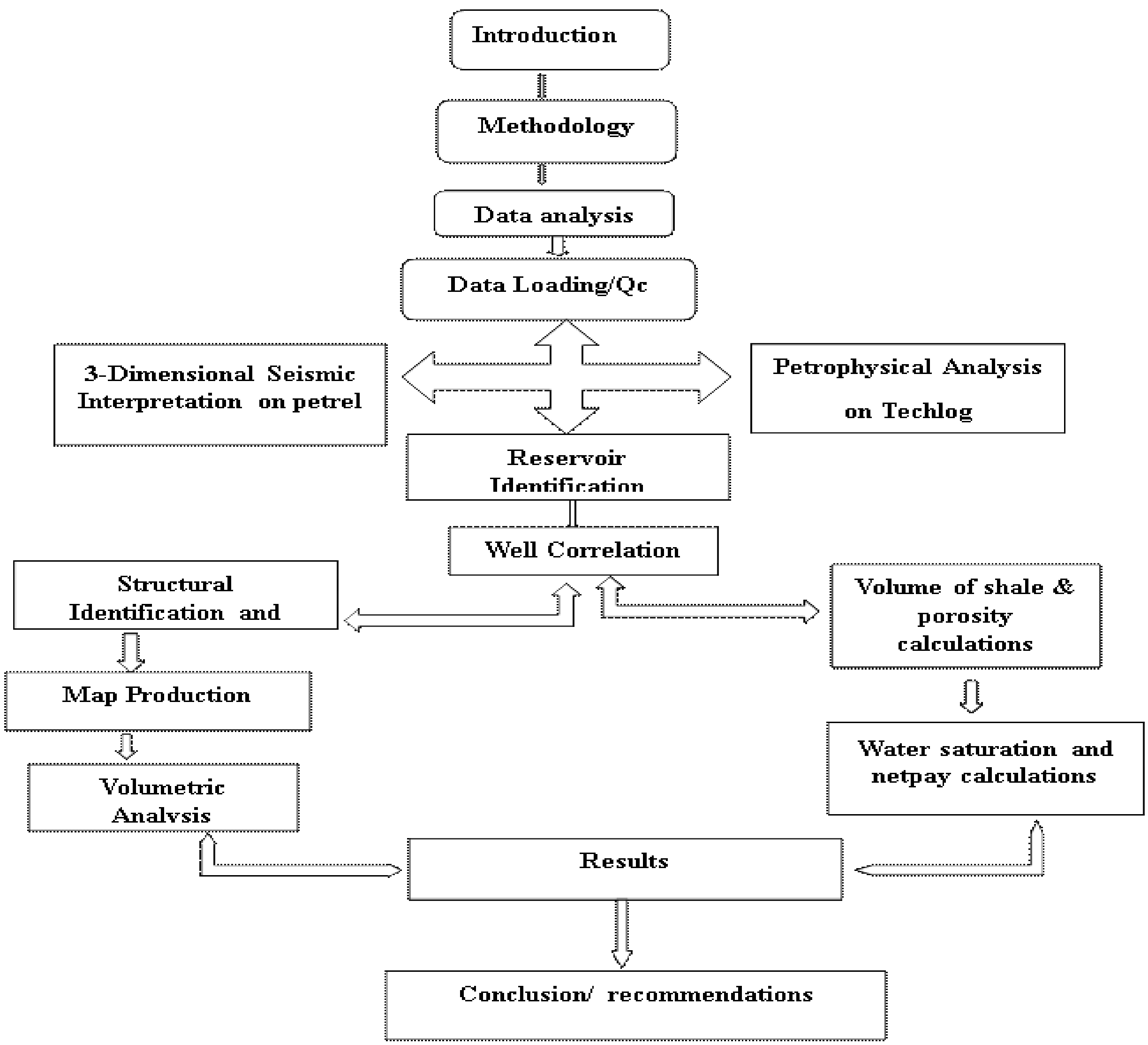

Fig. 3: Workflow designed for this research

2.2 Methodology

2.2.1 Lithologic Identification of Hydrocarbon-Bearing Sands

Lithology identification was determined using the composite well logs (gamma ray logs) to establish the formation's lithologies that the wells penetrated. These works are based on the fact that shale or clay minerals frequently have high gamma-ray signatures, because of their high content of radioactive elements such as uranium, potassium, zircon,(Alege, 2023) etc., while sand has low gamma-ray signatures (Alege, 2017). The unit was American Psychological Institute API ranging from 0-150API.

2.2.2 Well-log Correlation

Correlation is the determination of the continuity and age equivalence of rock units, particularly reservoir sands or marker-sealing shales, across a region of the subsurface (Embry, 2009). The determination of lateral continuity or Stratigraphic Interpretation of discontinuity of facies was accomplished using sand-to-sand/well-to-well correlation of hydrocarbon-bearing sands; this was done using the integration of Gamma Ray logs from the three wells based on their log motif or shapes as adopted from (Alege *et al*., 2022).

Petrophysical evaluation: first step taken in petrophysical analysis was the estimation of the Volume of Shale (Vsh). This was accomplished using a gamma ray log corrected with the Steiber function (Stieber, 1975), which is capable of indicating the smallest amount of shale in the Formation of a clean sandstone. Since the shale/clay minerals have a high content of radioactive materials, it is commonly accepted in practice to use the relative gamma-ray deflection as a clay volume indicator, and this principle was adapted for this work.

$$Linear\ Vsh = \left(\frac{GRlog-GRmin}{GRmax-GRmin}\right) \quad (1)$$

$$GRindex(X) = \frac{GRlog-GRmin}{GRmax-GRmin} \quad (2)$$

$$\text{Linear Vsh} = X \quad (3)$$

$$Clavier\ Vsh = 1.7\sqrt{3.38} - (X+0.7) \quad (4)$$

$$Steiber\ Vshale = 0\ \frac{0.5X}{1.5-X} \quad (5)$$

where the GR factor is a number chosen to force the result to imitate the behaviour of either the Clavier or the Stieber relationship (Clavier *et al.*, 2006).

Shale parameters (GRmin and GRmax) were determined using histogram analysis. Computation of Parameters used to determine Minimum and maximum GR values were sourced from the histogram plots.

2.2.3 Evaluation of porosity

This was done using the bulk-volume model of a clean formation with water-filled pore spaces (Walid and Ziad, 2020). Total porosity was estimated using a combination of neutron and density logs, whereby porosity decreases with increasing bulk density. The effective porosity was estimated from the total porosity by using the Volume of the shale to remove the effect of the shale.

Therefore, the bulk density (ρ_b) of the rock sample is derived from the empirical relation given as

$$\rho_b = \rho_{ma}(1-\varnothing) + \rho_f\varnothing \quad (6)$$

where (ρ_b) is the bulk density of rock, ρ_{ma} refers to the matrix density and $\rho_{f\varnothing}$ is the *refers* to the fluid density. A simple rearrangement of the terms leads to an expression for porosity:

$$\varnothing e = \varnothing_T - (\varnothing tsh \times Vsh) \quad (7)$$

with $\varnothing e$ refers to effective porosity, $\varnothing_T$ *refers* to total porosity and Vsh refers to Volume of shale.

2.2.4 ***Estimation of the water saturation step***

The Indonesian approach was chosen for the interpretation model of the shaly sands because it takes into consideration the impact of clay's presence in both heterolithic zones and the shaly sands and the fact that the formula accommodates freshwater parameter unlike Archie's equation.

$$SwI = \sqrt{\frac{1}{RT}} \div \frac{Vsh^{1-0.5\times Vsh}}{\sqrt{Rsh}+\sqrt{PHIE^{m/(a*Rw)}}} \ldots \text{eqn} \quad (8)$$

3-D seismic data analysis: This stage was accomplished by the application of the variance attribute approach, which is helpful in establishing the images of discontinuities in seismic data related to faults or stratigraphic sequences (Koson *et al.*, 2014).

2.2.5 Volumetric analysis

Gross rock volumes were calculated using the area of hydrocarbon accumulation obtained from the depth structural maps. The amount of oil and gas that were initially in place was developed and estimated using gross rock volume estimations and petrophysical characteristics based on the model in equation 9.

$$STOOIP = 7758 \times GRV \times NTG \times \Phi \times (Sh) \times \left(\frac{1}{Bo}\right) .. eqn \quad (9)$$

$$GIIP = 43560 \times GRV \times NTG \times \Phi \times (Sg) \times \left(\frac{1}{Bg}\right) \quad (10)$$

The symbols in the above equations are defined as follows: STOIIP = Stock Tank Oil Initially in Place, GIIP =Gas initially in Place, GRV= Gross Rock Volume defined by structure (Acre-ft.)

NTG= Net-to-Gross Ratio, Φ = Effective porosity (fraction), Sh= hydrocarbon Saturation (1-Sw), Bo= Oil formation volume Factor and Bg= Gas Formation Volume Factor.

3.0 Results and Discussion

Figs. 4 presents well log plots for the three wells while Tables 1 present information on the available log suits and the depth penetrated by each log.

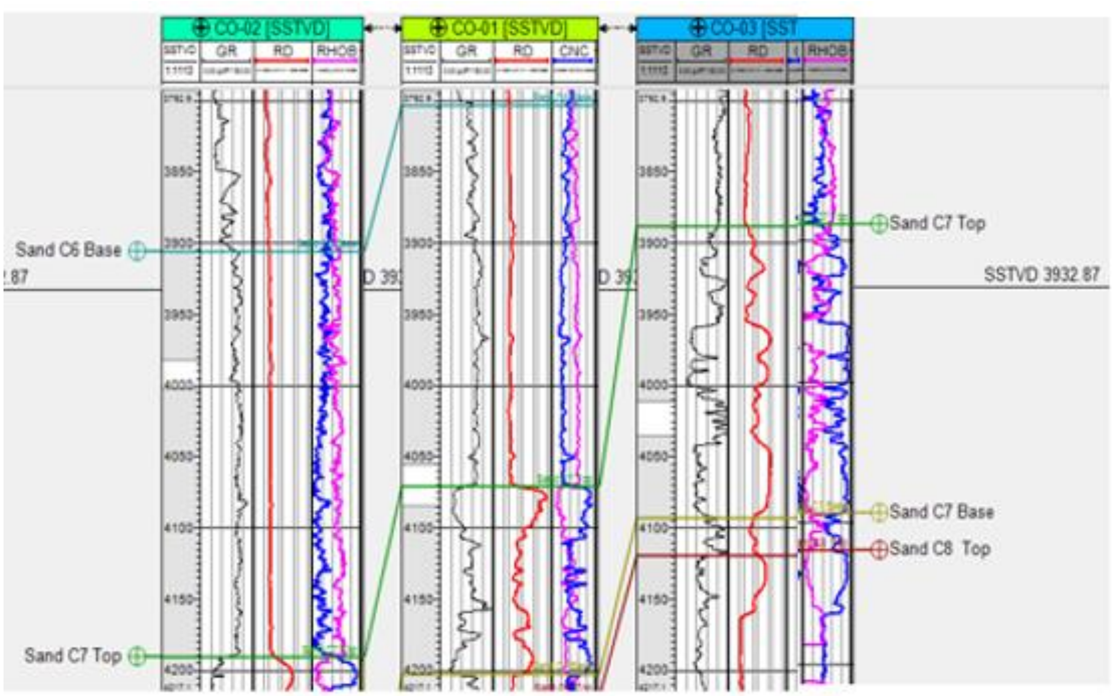

***Fig.* 4: the three well log plots**

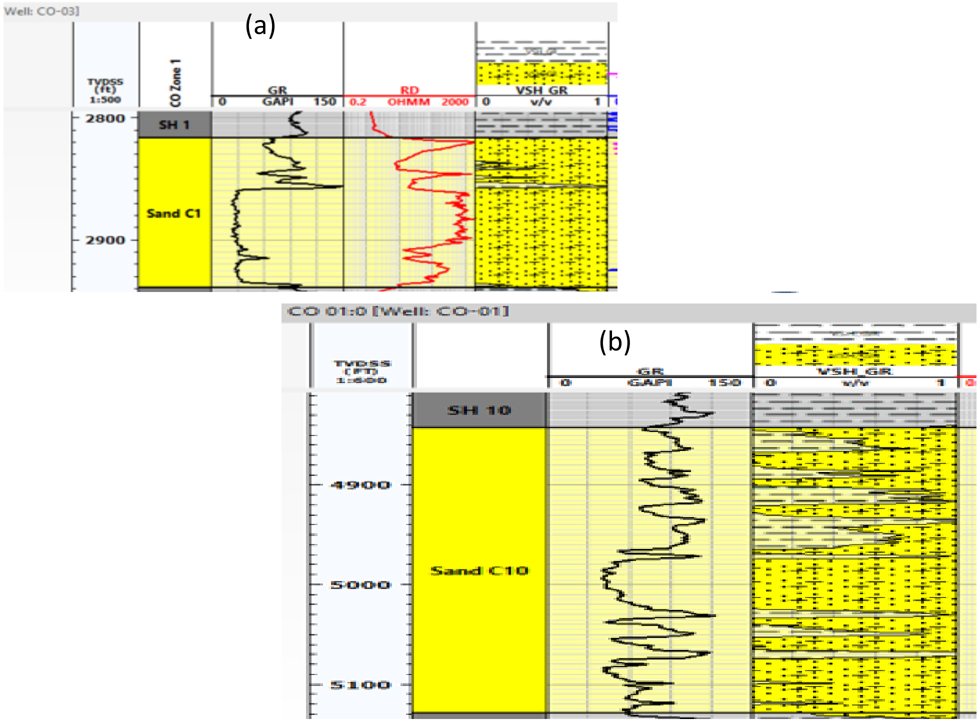

Fig. 5: shows Clean sandstone reservoir with low gamma ray, cylindrical shape (a) while (b) is sandstone reservoir with thinly bedded shale and has bell shape known as sandy shale/ silt stone.

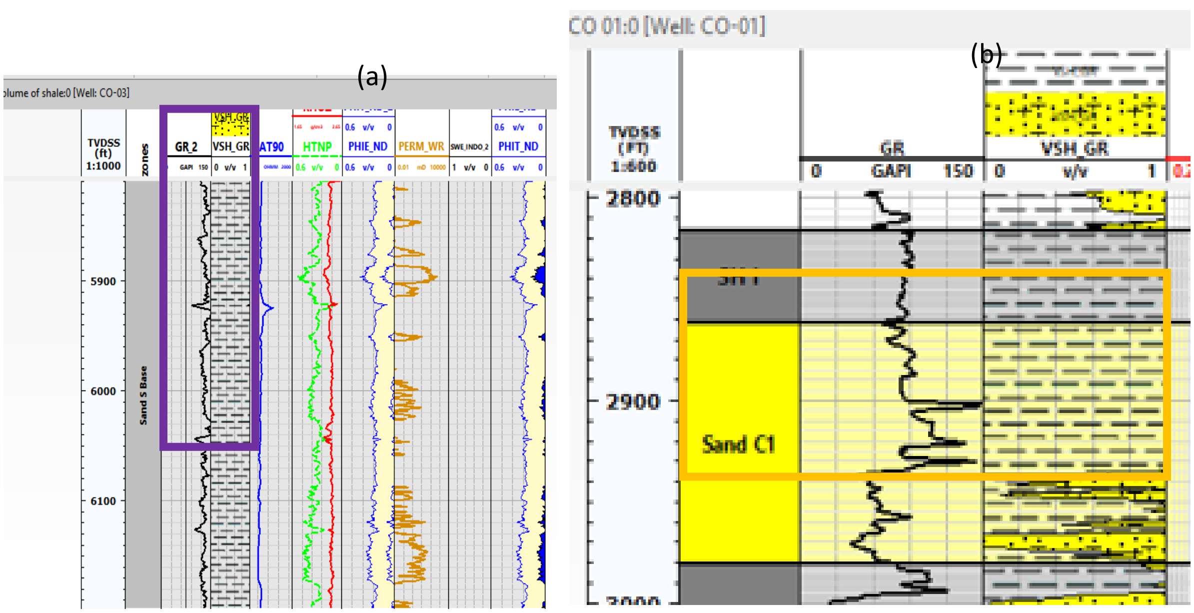

***Fig.* 6: This is a Shale unit with blocky shape as indicated in the blue rectangle (a), while (b) is a sandy shale (shale with small sandstone/ mud stone) is recognised by its serrated shape.**

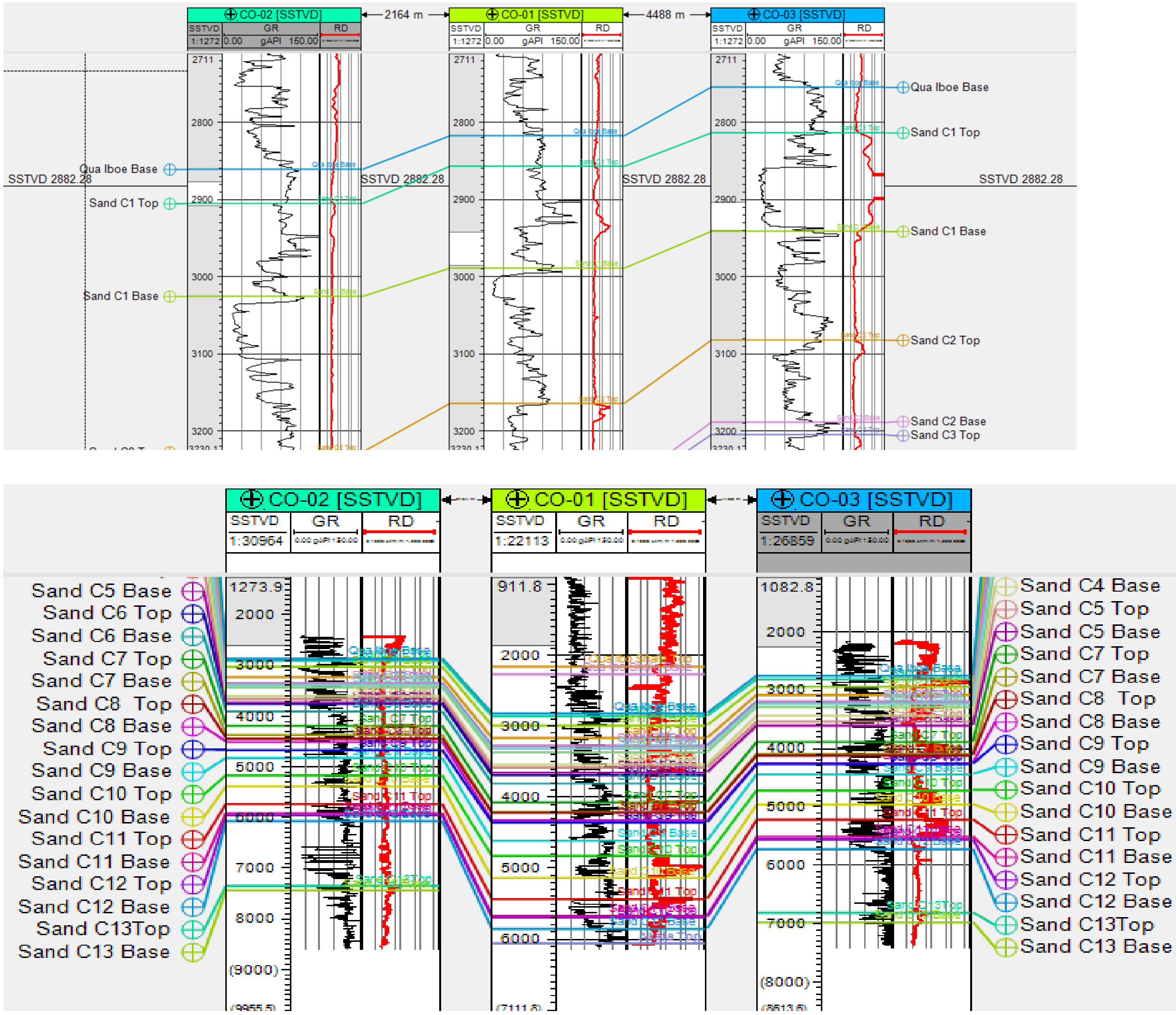

Fig. 7: well log correlation in Maboro-Field which shows that the reservoirs are continuous.

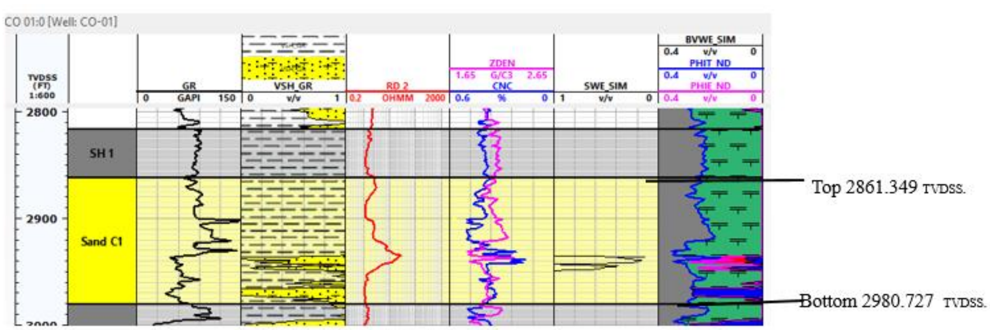

Well	Zones	Flag Name	Top	Bottom	Gross	Net	Net to Gross	Av_Porosity	Av_Water Saturation
CO-01	Sand C1	RES	2861.349	2980.727	119.378	18	0.151	0.227	0.695
CO-01	Sand C1	PAY	2861.349	2980.727	119.378	9.5	0.08	0.19	0.338

Fig. 8: The sand CO-01 C1 reservoir is a shaly sand with good resistivity value, poor porosity, moderate water saturation and the Neutron Density cross over indicates a small Gas.

From this Fig. it is evident that the CO-01 C1 reservoir is highly compacted and can affect the productivity.

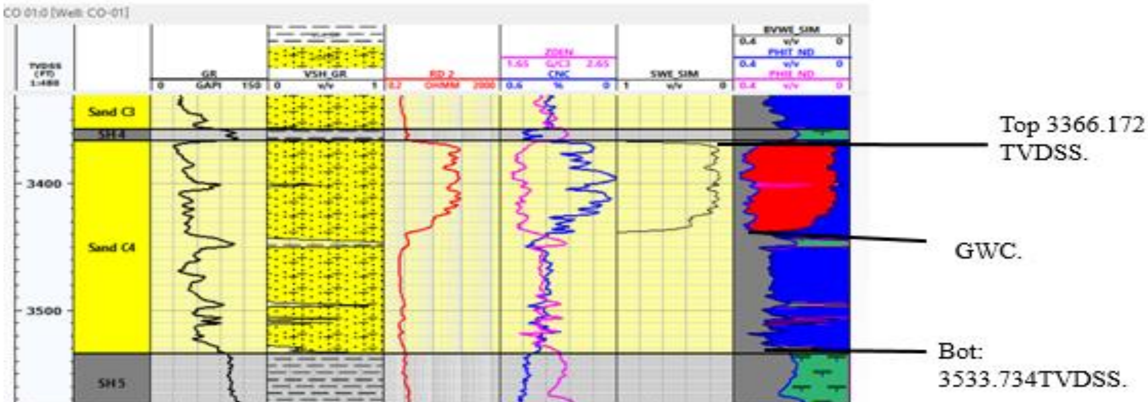

Well	Zones	Flag Name	Top	Bottom	Gross	Net	Net to Gross	Av_Porosity	Av_Water Saturation
CO-01	Sand C4	RES	3366.172	3533.734	167.563	155	0.925	0.297	0.59
CO-01	Sand C4	PAY	3366.172	3533.734	167.563	70	0.418	0.34	0.208

***Fig.* 9: Sand C4 is a good reservoir sand from the gamma ray log, resistivity value indicates that there is fluid, using neutron –density crossover indicates that there is gas. The water saturation and porosity (both total and effective) value is good.**

The application of gamma-ray logs for lithology identification aligns with established practices (Alege *et al*., 2020b). The differentiation of sandstone, shale-rich sandstone, sand-rich shale, and shale (Ajogwu *et al*., 2023) is crucial for reservoir characterization. Studies suggest that effective porosity and permeability are generally lower in shaly formations due to the presence of clay minerals that can restrict fluid flow (Walid & Ziad, 2020). The well log correlation indicating lateral continuity of thirteen potential hydrocarbon-bearing sands (Ajogwu *et al*., 2023) is a positive finding. Reservoir continuity is a critical factor for efficient hydrocarbon production as it allows for better well drainage (Alege, 2022).

The estimation of porosity using a combination of neutron and density logs (Ajogwu *et al*., 2023) aligns with common practices (Walid & Ziad, 2020). The observed variations in gamma-ray signatures suggest that some zones may have good porosity and hydrocarbon saturation (*Fig.* 9, Ajogwu *et al*., 2023). This aligns with expectations, as lower gamma-ray readings typically correspond to cleaner sandstone with higher porosity potential (Alege *et al*., 2020a). Conversely, zones with high shale content and potentially lower porosity may be reflected in higher gamma-ray readings (Fig. 8, Ajogwu *et al*., 2023). This observation is supported by (Walid and Ziad, 2020) who highlight the negative impact of shale content on porosity.

The Indonesian equation employed for water saturation estimation in shaly sands (Ajogwu *et al*., 2023) is a well-established approach compared to Archie's equation, which can underestimate water saturation in such formations (Walid & Ziad, 2020).

3.1 Volumetric analysis and production potential

The volumetric analysis, though not explicitly shown in the excerpt, likely considered factors like net-to-gross ratio, effective porosity, and hydrocarbon saturation (Ajogwu *et al*., 2023) as suggested by Equations 9 and 10. This approach aligns with conventional practices for estimating Stock Tank Oil Initially In Place (STOOIP) and Gas Initially In Place (GIIP) (Press & Raymond, 2003). The possibility of significant gas reserves in some reservoirs based on the workflow (Ajogwu *et al*., 2023) warrants further investigation.

2.2 Integration with 3D seismic data

The utilization of 3D seismic data and the variance attribute method for structural interpretation (Ajogwu *et al*., 2023) is a valuable addition to the analysis. Seismic data can provide insights into potential hydrocarbon traps and reservoir geometries that cannot be directly obtained from well logs (Eshimokhai & Akirevbulu, 2012). The observed favorable structural conditions for hydrocarbon accumulation based on 3D seismic data (Ajogwu *et al*., 2023) are encouraging. Favorable structural features, coupled with good reservoir characteristics identified in some zones, suggest potential for hydrocarbon production in the Maboro-Field.

In Taable 2, a summary for petrophysical Analysis in CO-01 is shown. The CO-01 well exhibits significant gross thickness in zones like Sand C2 (191.97m), Sand C4 (167.563m), and Sand C5 (70.324m), indicating robust reservoir potential. The net thickness values, while high in some zones (e.g., Sand C2 with 122.79m), show that only a portion of these zones is effective reservoir rock. Pay zones, which represent producible hydrocarbons, are notably smaller (e.g., Sand C2 with 76.26m net pay).Average porosity values are relatively high, ranging from 19% to 40%, which suggests good reservoir quality. However, Water saturation values vary significantly, with some zones exhibiting high water saturation (e.g., Sand C6 with 96.6% in RES), potentially indicating challenges in hydrocarbon extraction. The findings align with literature emphasizing the importance of porosity and net-to-gross ratio in evaluating reservoir quality. High porosity and low water saturation typically correlate with better hydrocarbon production potential (Clarkson & Solano, 2022).

In Table 3 a summary for Petrophysical Analysis in CO-02 is presented, From the results shown in the Table, Sand C5 and C7 in the CO-02 well have gross thicknesses of 72.495m and 181.02m, respectively, but exhibit lower net-to-gross ratios compared to CO-01. The net thicknesses for pay zones are relatively low, such as 11.205m for Sand C5 and 23.195m for Sand C7, indicating limited producible hydrocarbons. The average porosity for Sand C5 and C7 is around 38% and 34%, respectively, indicating favorable reservoir quality. However, the water saturation values are high (up to 87.2% in Sand C5 RES), which suggests potential high water cut in production. High water saturation could be problematic for hydrocarbon production, necessitating enhanced recovery techniques (Gao & Li, 2021). This aligns with the literature that highlights the need for advanced water management strategies in reservoirs with high water saturation (Jafari & Nasriani, 2020).

A Summary for Petrophysical Analysis in CO-03 is shown in Table 4. From the results, we observed that zones such as Sand C1 and C4 exhibit high gross and net thicknesses (e.g., Sand C1 with 122.995 m gross and 116.436 m net), indicating substantial reservoir capacity. Pay zones are significant, with Sand C1 having a pay thickness equal to its net thickness, showing a good balance between total reservoir and producible hydrocarbon volume. The average porosity values are generally favorable, around 35-39%, suggesting good reservoir quality. The water saturation varies significantly, with some zones like Sand C2 having very high water saturation (92.8% in RES), posing potential challenges for production. From the literature, High net-to-gross ratios in well CO-03 indicate effective reservoir rock presence, essential for economic hydrocarbon extraction (Hosseini & Rahimpour-Bonab, 2019). However, managing high water saturation is crucial for optimizing production.

Table 5 provides a summary of volumetric results. From the information, provided in the Table, the reservoirs have substantial gas-in-place (GIIP) volumes, with significant contributions from zones like C10 (305.12 BCF) and C11 (388.55 BCF). Oil volumes are smaller but still notable, particularly in C7 (18.17 MMSTB). Parameters such as gross rock volume (GRV), net-to-gross ratio (NTG), porosity, and water saturation (SW) are used to estimate these volumes, reflecting good reservoir properties. Also, the volumetric analysis suggests a robust potential for gas production, consistent with findings in similar geological settings where high porosity and favorable net-to-gross ratios are linked to significant hydrocarbon volumes (Dutta *et al*., 2020). However, high water saturation in some zones may require innovative extraction techniques to maximize recovery.

The petrophysical analysis of the CO-01 and CO-03 wells indicates substantial hydrocarbon potential, with favorable porosity and net-to-gross ratios in many zones. While the CO-02 has low hydrocarbon production performance due to high water saturation, high volume of shale and poor porosity in certain intervals which presents a challenge for efficient hydrocarbon extraction. This underscores the need for advanced reservoir management and recovery techniques to optimize production. The volumetric analysis confirms significant gas-in-place volumes, indicating the economic viability of the field.

Table 2: Summary Table for Petrophysical Analysis in CO-01

Well	**Zones**	**Flag Name**	**Top**	**Bottom**	**Gross**	**Net**	**Net to Gross**	**Av_Porosity**	**Av_Water Saturation**
CO-01	C1	RES	2921.07	2982.37	61	42	70	20	083
CO-01	C1	RES	2921.07	2982.37	61	10	16	21	0.40
CO-01	Sand C2	RES	2857.05	3049.02	191.97	122.79	0.64	0.28	0.44
	Sand C2	PAY	2857.05	3049.02	191.97	76.26	0.64	0.30	0.15
	Sand C4	RES	3366.172	3533.734	167.563	155	0.925	0.297	0.59
	Sand C4	PAY	3366.172	3533.734	167.563	70	0.418	0.34	0.208
	Sand C5	RES	3581.485	3651.81	70.324	56.5	0.803	0.311	0.383
	Sand C5	PAY	3581.485	3651.81	70.324	51	0.725	0.323	0.351
	Sand C6	RES	3689.576	3802.008	112.432	112	0.996	0.253	0.966
	Sand C6	PAY	3689.576	3802.008	112.432	6.5	0.058	0.317	0.57
	Sand C7	RES	4068.112	4203.985	135.874	84.485	0.622	0.292	0.283
CO-01	Sand C7	PAY	4068.112	4203.985	135.874	78	0.574	0.304	0.258
	Sand C9	RES	4351.146	4611.316	260.171	119	0.65	0.19	0.957
Well	Zones	Flag Name	Top	Bottom	Gross	Net	Net to Gross	Av_Porosity	Av_Water Saturation
	Sand C9	PAY	4351.146	4611.316	260.171	7.5	0.56	0.21	0.58
	Sand C10	RES	4842.836	5128.619	285.783	186.119	0.651	0.274	0.337
CO-01	Sand C10	PAY	4842.836	5128.619	285.783	163.5	0.572	0.283	0.286

Sand C11	RES	5436.107	5668.532	232.425	154.5	0.665	0.234	0.58
Sand C11	PAY	5436.107	5668.532	232.425	69.5	0.299	0.277	0.283
Sand 12	RES	5693.854	5854.833	160.979	138.5	0.86	0.20	0.85
Sand 12	PAY	5693.854	5854.833	160.979	29	0.18	0.19	0.60

Table 3: Summary Table for Petrophysical Analysis in CO-02.

Well	Zones	Flag Name	Top	Bottom	Gross	Net	Net to Gross	Av_Porosity	Av_Water Saturation
CO-02	Sand C5	RES	3655.717	3728.211	72.495	49.085	0.677	0.403	0.872
CO-02	Sand C5	PAY	3655.717	3728.211	72.495	11.205	0.155	0.38	0.492
	Sand C7	RES	4187.924	4368.943	181.02	85.317	0.471	0.341	0.783
	Sand C7	PAY	4187.924	4368.943	181.02	23.195	0.128	0.387	0.308

Table 4: Summary Table for Petrophysical Analysis in CO-03

Well	Zones	Flag Name	Top	Bottom	Gross	Net	Net to Gross	Av_Porosity	Av_Water Saturation
CO-03	Sand C1	RES	2816.13	2939.125	122.995	116.436	0.947	0.351	0.187
CO-03	Sand C1	PAY	2816.13	2939.125	122.995	116.436	0.947	0.351	0.187
	Sand C2	RES	3085.634	3191.898	106.264	102.927	0.969	0.387	0.928
	Sand C2	PAY	3085.634	3191.898	106.264	14.153	0.133	0.353	0.442
	Sand C3	RES	3206.368	3272.84	66.471	65.376	0.984	0.376	0.948
	Sand C3	PAY	3206.368	3272.84	66.471	4.481	0.067	0.389	0.561
	Sand C4	RES	3284.126	3444.31	160.183	140.814	0.879	0.386	0.706
	Sand C4	PAY	3284.126	3444.31	160.183	56.985	0.356	0.399	0.33
	Sand C7	RES	3888.394	4100.235	211.841	98.363	0.464	0.315	0.185
	Sand C7	PAY	3888.394	4100.235	211.841	97.48	0.46	0.315	0.179
	Sand C8	RES	4109.351	4254.341	144.99	111.31	0.768	0.279	0.797
	Sand C8	PAY	4109.351	4254.341	144.99	29.813	0.206	0.292	0.286
	Sand C9	RES	4268.667	4430.441	161.774	61.833	0.382	0.238	0.943
	Sand C9	PAY	4268.667	4430.441	161.774	7.174	0.044	0.238	0.519
	Sand C10	RES	4727.076	4965.832	238.755	21.317	0.089	0.192	0.197
	Sand C10	PAY	4727.076	4965.832	238.755	20.447	0.086	0.194	0.182
	Sand C11	RES	5222.675	5512.979	290.304	159.775	0.55	0.28	0.26
	Sand C11	PAY	5222.675	5512.979	290.304	159.775	0.55	0.28	0.24
	Sand 12	RES	5580	5710	170.979	112.5	0.85	0.28	0.85
	Sand 12	PAY	5693.854	5854.833	160.979	29	0.18	0.26	0.38

Figure 9 shows a 3-D Seismic view of the area covered by Maboro field This figure provides an area overview of the Maboro-Field, depicting the extent covered by the 3D seismic data (99.9 Km^2) using inline, crossline, and time-slice displays. This information is essential for understanding the spatial coverage of the seismic survey and its relation to the wells used in the study. In Fig. 10, the seismic section with faults is shown. This figure shows a seismic section with NW-SE trending faults labeled F1 and F2. These faults are major features that can influence hydrocarbon accumulation by creating traps as aligned with (Alege *et al*., 2017) which stated that faults can serve as pathways for upward migration of hydrocarbon generated within an underlying shale.. The presence of faults can be positive if they juxtapose impermeable and permeable formations, creating a reservoir seal (Press & Raymond, 2003). However, faults can also act as conduits for fluid migration if not properly sealed. Further analysis is needed to determine the specific role of these faults in the Maboro-Field.

Fig. 10 shows a seismic section with NW-SE trending faults labeled F1 and F2. These faults are major features that can influence hydrocarbon accumulation by creating traps. The presence of faults can be positive if they juxtapose impermeable and permeable formations, creating a reservoir seal (Alege, 2017). However, faults can also act as conduits for fluid migration if not properly sealed. Further analysis, such as fault throw and juxtaposition relationships, is needed to determine the specific role of these faults in the Maboro-Field. Integration of the fault interpretation with the well data can reveal if the faults displace the reservoir zones and impact fluid.

Fig.s 11 and 12 demonstrate the process of converting seismic data from two-way travel time, used for seismic imaging, to depth, a critical step for reservoir characterization in the Maboro-Field..

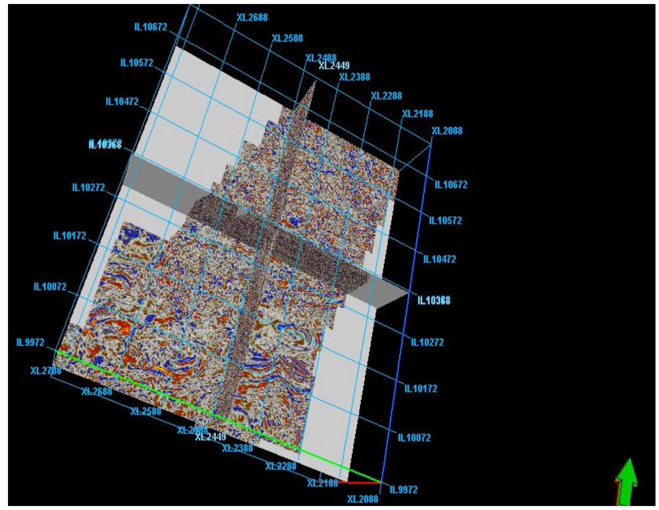

Fig. 9: 3-D seismic section showing Area extent (inline, crossline and time-slice) covered by Maboro-Field 99.9 K

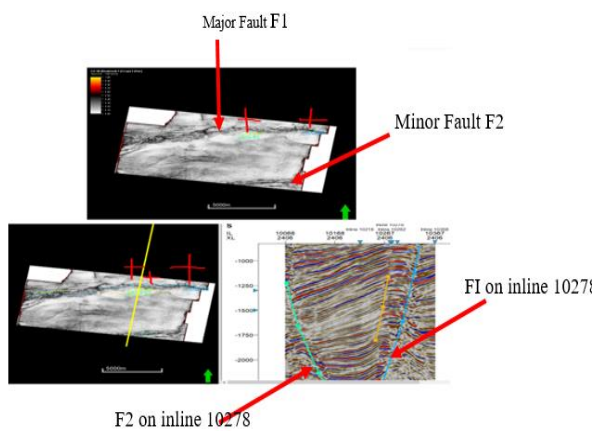

Fig.s 10: Seismic section showing the NW-SE trending fault (F1& F2) major fault that host hydrocarbon in Maboro-Field.

Fig. 11 shows a seismic time slice extracted from the 3D seismic data volume. A specific seismic horizon, likely corresponding to the top of the sand C2 reservoir, is interpreted and displayed as a colored line or surface. This horizon represents a seismic reflection interface that marks the boundary between different geological layers. Variations in the two-way travel time to the interpreted horizon are inferred from the color variations on the time map. Cooler colors (e.g., blue) might represent deeper sections, while warmer colors (e.g., red) indicate shallower sections of the horizon. According to Avseth, Mukerji, and Mavko (2010), the interpretation of seismic horizons and their color variations can reveal structural features and potential hydrocarbon traps.

Fig. 12 depicts the model used to convert the two-way travel time data (from *Fig.* 11) to depth. This model considers factors such as the seismic velocity profile within the subsurface layers, which is derived from well logs (e.g., sonic logs) that measure the actual seismic velocity in rock formations. By applying this model to the two-way travel time data, geophysicists estimate the actual depth of the interpreted horizon (sand C2 reservoir top) across the entire seismic survey area. The conversion of seismic data from time to depth using velocity profiles is a standard practice in geophysical exploration, as highlighted by Yilmaz (2001).

*Fig.*s 11 and 12, when used together, allow for the identification of the top of the sand C2 reservoir based on seismic reflections. The depth conversion model (*Fig.* 12) transforms the variations in two-way travel time from *Fig.* 11 into a depth map, depicting the actual depth variations of the reservoir top across the surveyed area. The significant of depth mapping are accurate well planning and targeting, reservious volume estimation and understanding of reserviour geometry

Fig. 11 demonstarted a relative depth picture of the C2 reservoir based on two-way travel time variations. Warmer colors indicate shallower travel times, potentially suggesting structural highs that might trap hydrocarbons. Conversely, cooler colors represent deeper travel times, indicating lows. *Fig.* 12 (Conversion Model) Acts as the bridge between the time map and the depth map. It shows the seismic velocity profile (Vs), likely obtained from a vertical seismic profile (VSP) well. Using the Vs profile and the equation Depth = Velocity x Time, geophysicists convert travel times from the time map into actual depths for the C2 reservoir top. *Fig.* 13, derived from *Fig.*s 11 and 12, displays the actual depth to the top of the C2 reservoir across the field. By analyzing color variations (depth variations), the depth map reveals structural features ***to include the following***

(i) Structural Highs (Domes): Warmer colors and closed contours indicate shallower depths and potential hydrocarbon traps. These are prime targets for well placement.
(ii) Structural Lows (Depressions): Cooler colors and closed contours represent deeper zones, which might also hold hydrocarbons depending on other factors (e.g., pressure).
(iii) Dips and Slopes: The overall color trends and gradients reveal the dip and slope of the reservoir top, influencing fluid flow within the reservoir.
(iv) Structural mapping using seismic data and depth conversion models is essential for identifying optimal drilling locations and understanding reservoir architecture (Brown, 2011).

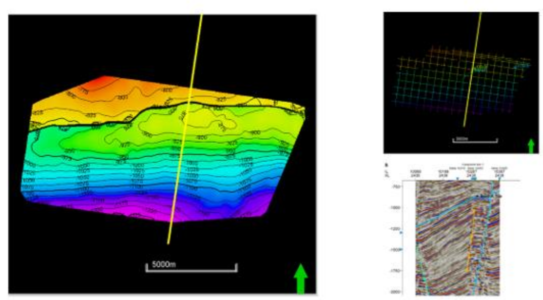

***Fig.*s 11: Horizon interpretation and time map generated from sand C2 reservoir of Maboro-Field.**

The depth map (Fig. 13) identifies structural highs (domes) as priority locations for well placement due to their higher potential for trapping hydrocarbons. Targeting structural highs is a proven strategy for optimizing hydrocarbon extraction (Telford *et al*., 1990).: Depth information from *Fig.* 13 should guide decisions about wellbore trajectory and drilling depths. Knowing the depth to the reservoir top allows for efficient planning and cost-effective well construction**.** Efficient planning and wellbore trajectory optimization are critical for maximizing production efficiency and reducing costs (Fanchi, 2010). **.**

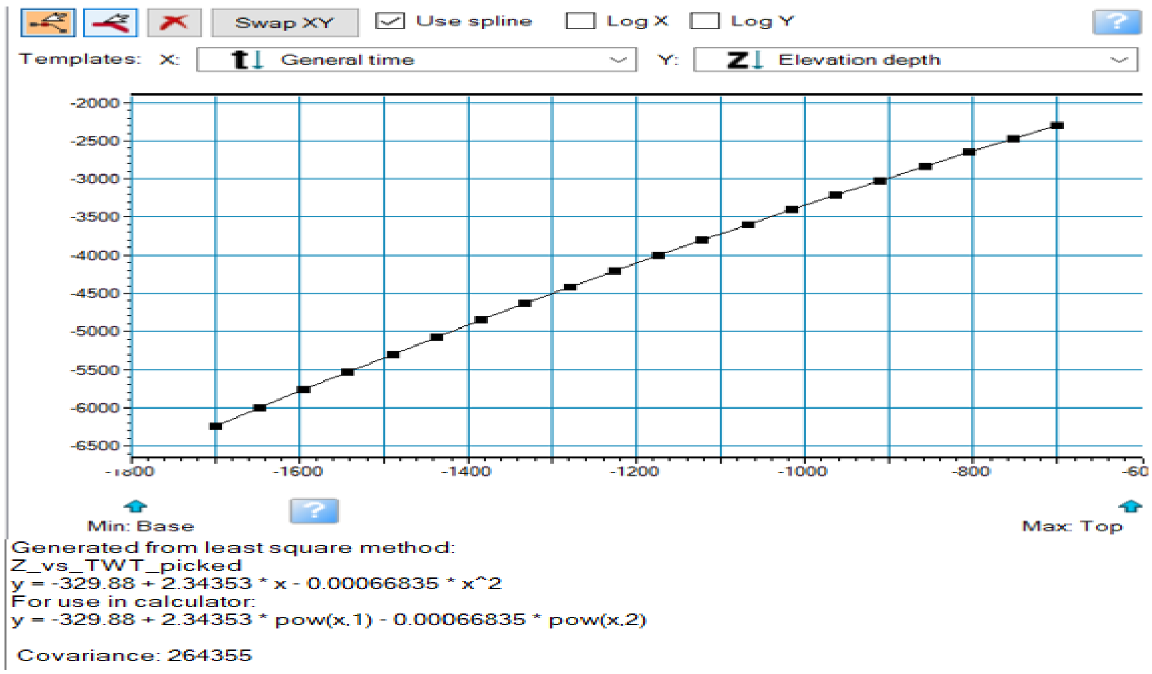

***Fig.* 12: Depth conversion model, the two-way time used to convert time map to depth**

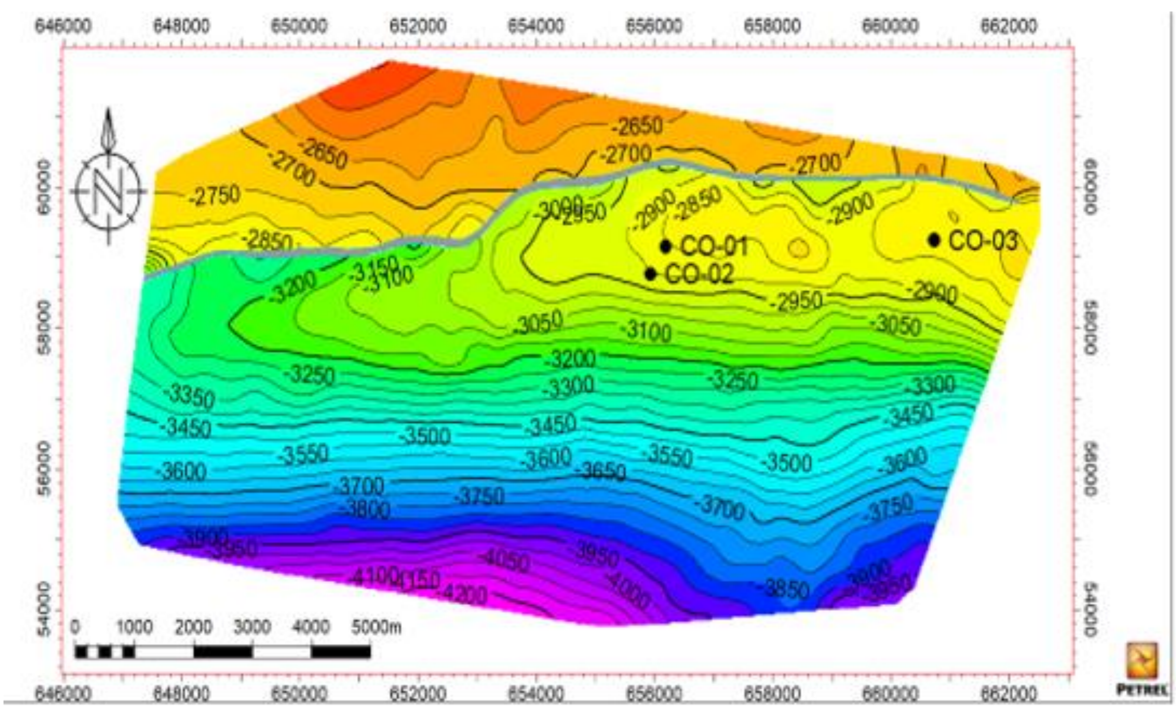

***Fig.* 13: Generated depth map from sand C2-reservoir of Maboro -Field.**

Table 5: Summary of Volumetric results

RESERVIOR	FLUID	GRV	NTG	POROSITY	SW	BG [(CF/SCF)/BO(RB/STB)]	GIIP(BCF)	STOOIP (MMSTB)
C1	Gas	237,060	0.90	0.29	0.26	0.0092	216.79	
C2	GAS	140,646	0.95	0.35	0.44	0.0089	128.18	
C3	GAS	6,108	0.95	0.38	0.56	0.0086	4.91	
C4	GAS	160,619	0.88	0.36	0.27	0.0086	188.15	
C5	GAS	120,493	0.73	0.32	0.35	0.0086	92.67	
C7	GAS	335, 398	0.54	0.32	0.22	0.0086	228.98	
	OIL	18,768	0.54	0.32	0.22	1.0800		18.17
C8	GAS	22,892	0.77	0.29	0.29	0.0067	23.60	
C10	GAS	459,324	0.51	0.24	0.24	0.0061	305.12	
C11	GAS	462,264	0.67	0.24	0.28	0.0060	388.55	
C12	GAS	226,306	0.85	0.26	0.38	0.0056	241.20	
						Total	1818.13	18.17

4.0 Conclusions

This study focuses on the petrophysical evaluation of reservoir sands in Well CO-01, CO-02 and CO-03 OF Maboro field. The key petrophysical parameters—gross thickness, net-to-gross ratio, average porosity, and water saturation—were assessed to determine the reservoir quality and hydrocarbon potential. The analysis reveals that most of the reservior sands exhibit favo***u***rable characteristics, with high net-to-gross ratios and substantial porosity. Sand C1 is identified as the most promising interval due to its highest net-to-gross ratio (0.85) and lowest water saturation (25%).

The petrophysical analysis of Well CO-01 demonstrates significant hydrocarbon potential in the analyzed sands. The results indicated that all the sands exhibit high net-to-gross ratios, indicating a high proportion of reservoir rock, which is essential for effective hydrocarbon extraction. The porosity values range from 20% to 25%, suggesting good to very good storage capacity for hydrocarbons. However, lower water saturation in sands B3 and C1 indicates higher hydrocarbon saturation, enhancing their production potential.

The study confirms that Well CO-01 and CO-03 contains high-quality reservoir sands, with Sand C1 and C7 emerging as the most favourable interval for hydrocarbon production due to its superior petrophysical properties. In view of the observed results and findings from the present study, the following recommendations are made.

(i) Given their high net-to-gross ratios, substantial porosity, and low water saturation, these sands should be the primary targets for hydrocarbon extraction to maximize production efficiency and yield.
(ii) For sands with higher water saturation, it is crucial to develop and implement advanced water management techniques to mitigate the impact on hydrocarbon recovery.
(iii) Regular monitoring of reservoir performance and periodic re-evaluation of petrophysical properties should be conducted to adjust production strategies and ensure optimal recovery.
(iv) Complementary studies, including seismic surveys and geological modeling, should be undertaken to enhance the understanding of the reservoir's structural and stratigraphic framework, supporting more accurate predictions of hydrocarbon distribution and movement.
(v) Hydraulic fracking is also crucial in a tight reservoir for enhanced oil recorvery.

5.0 References

Ahmad, N., Al-Harthy, A., & Al-Mahrooqi, S. (2022). Advances in Petrophysical Analysis: Applications in Reservoir Characterization. *Journal of Petroleum Science and Engineering*, 209, 109993, doi: 10.5772/26404.

Alege, T. S. (2017). Sequence stratigraphy of Akos Field using well logs, Coastal Swamp Depobelt of the Niger Delta: *Advanced Applied Science Research*, 8, 1, pp. 16-27.

Alege, T. S. (2017). Structural interpretation of 3D seismic Data of Akos Field in the Coastal Swamp Depobelt of the Niger Delta. *International Journal of Research and Innovations in Earth Science*, 4, 2, pp. 68-77.

Alege, T. S. (2022). Sequence stratigraphic evaluation of sediments domicile in day field located in the Onshore central Swamp Depobelt of the Niger Delta: j*ourna of applied science Environmental management, 26, pp.* 1129-1135. https://doi.org/10.4314/ jasem volume 26/6.

Alege, T. S. Adamu, M. L. and Odoma, A. N. (2020b). sedimentology, lithofacies, palynofacies and sequence stratigraphy of the Campano-Maas-trichtian successions within the Southern Bida Basin Nigeria. Min J Geos MJG4(2): 122-142 *Petroleum Technology Development.* 10, 1, pp. 14-26.

Alege, T. S. Joseph I. O. and Onimisi, M. (2020a). Lithofacies and Environmental Interpretation of Akos Field using well logs, Coastal Swamp Depobelt of the Niger Delta: *Petroleum Technology Development Journal Volume.* 10, 1, pp. 14-26.

Alege, T. S., *et al*. (2020). Petrophysical evaluation of hydrocarbon-bearing formations: A review of methods and applications. *Journal of Petroleum Exploration and Production Technology*, 10, 5, pp. 2311-2327.

Alege, TS., Tella, TO., Aigbadon GO., and Omada, JI. (2023). Sedimentary facies and palynological studies of ajali sandstones formation outcropping in Idah Northern Anambra Basin, Nigeria. Journal of Applied Science Environmental Management 27, 6, pp. 1207-1215.

Auduson, A. E. (2018). *Borehole geophysics: An introduction.* Wiley-Blackwell.

Auduson, A. E. (2018). *Concise Applied Geophysics, a practical approach Delizon publishers first edition*, pp 11Delison Publisher, Nigeria.

Auduson, A. E. (2022) *Reservior Geology Lecture notes unpublished*, page 54.

Avseth, P., Mukerji, T., & Mavko, G. (2010). *Quantitative seismic interpretatioApplying rock physics tools to reduce interpretation risk*. Cambridge University Press.

Brown, A. R. (2011*). Interpretation of three-dimensional seismic data (7th ed.).* AAPG Memoir.

Claverier, M., Aboel A., Harfoushian H., Hansen S. & Leech, R. (2006). *Methods for formation evaluation and formation testing of thinly bedded reservoirs*. 'SPE Asia Pacific Oil and Gas Conference and Exhibition'. Held 9-14.

Corredor, F., Shaw, J. H. & Bilotti, F. (2005), Structural styles in the deep-water fold and thrust belts of the Niger Delta. *American Association of Petroleum Geologists Bulletin*, 89, pp. 753-780.

Craft, B. C., & Hawkins, M. F. (1991). *Applied petroleum reservoir engineering. Prentice Hall.*

Dharmmattan Nigeria Limited (1997). *In field lecture report Offshore Niger Delta Basin* unpublished pp (10-200).

Doust, H. and Omatsola, E. (1990). Niger Delta, in, Edwards, J. D. & Santogrossi, P.A., eds., Divergent/ passive Margin Basins, AAPG Memoir 48: Tulsa, American Association of Petroleum Geologists, in Ighodaro, *et al* edition, (2019). Petrophysical Evaluation of Reservoir in X-Field Niger Delta. *Journal of Applied. Science and Environmental. Management*t, 23, 5, pp. 917-925. Doi: https://dx.doi.org/10.4314/jasem.v23i5.23.

Embry, A. F., (2009). *Practical Sequence Stratigraphy. Canadian Society of Petroleum Geologists*, p. 67-75 retrieved from http://www.cspg.org.

Eshimokhai, J., & Akirevbulu, S. (2012). Integrated petrophysical evaluation of reservoirs: A case study of XYZ field, Niger Delta. *Journal of Petroleum Exploration and Production Technology*, 2, 2, pp. 69-78.

Eshimokhai, S. & Ankirevbulu, O. E. (2012). Reservoir characterization using seismic and well log data (A case study of Niger Delta). *Ethiopian Journal of Environmental Studies and Management*, 5, 4, .http://dx.doi.org/10.4314/ejesm.v5i4.S20.

Fanchi, J. R. (2010). Integrated reservoir asset management: Principles and best practices. Gulf Professional Publishing.

Koson, S., Piyaphong, C. & Montri, C. (2014). Enhancing *Geological Interpretation with Seismic Attributes in Gulf of Thailand*. B.Sc. report, Chulalongkorn University Thailand, pp 6.

Lake, L. W. (1989). *Enhanced oil recovery*. Prentice Hall.

Lee, J., & Horne, R. (2021). *Petrophysics: Fundamentals and Applications*. Elsevier.

Mobeen, M., Sami, A. N. & Asmar, W. (2013). *Design and Evaluation of Hydraulic Fracturing in Tight Gas Reservoirs SPE Saudi Arabia Section Technical Symposium and Exhibition*, Al-Khobar, Saudi Arabia: SPE-168100-MS.

Muhammad, N; Muhammad, K.J; Sayed, S.RM., Nassir, SA; Shazia, A.; Farhan, K. & Nisar, A. (2015); Seismic and well-log driven structural and petrophysical analysis of the Lower Goru Formation in the Lower Indus Basin. Pakistan: Geoscience Journal, in Eshimokhai, S. and Ankirevbulu, O. E., (2022). Reservoir characterization using seismic and well log data (A case study of Niger Delta). OI: doi.org/10.4314/jasem.v26i5.20.

Nton, M. E. & Ogungbemi, TS. (2011). Sequence stratigraphic framework of K-Field in part of western Niger Delta: RMZ-Materials and Geoenv. Journal of

Applied Science Environmental Management 58, 2, pp. 163-180

Nwajide, C. S., Ekwenye, O. C., Nichols, G.J., Collinson, M. & Obi, G.C. (2005). A paleogeographic model for the sandstone members of the Imo Shale, south-eastern Nigeria, Journal of African Earth Science volume 96, 3, doi.org/10.1016/j.jafrearsci.2014.01.007.

Peter, B. & Amandeep, K. (2013). *Effective Fault Interpretation using 3-D Software Technology and Fault Displacement Analysis in Ugwu* edition 2020: T ISSN 1119-8362.

Press, F. &Raymond S. (2003). *Energy and mineral resources from Earth in understanding earth*. Freeman publishers ISBN 10: 0716796171 - ISBN 13: 9780716796176.

Press, F., & Raymond, C. (2003). *Introduction to petroleum exploration and engineering*. Elsevier.

Schlumberger. (2013). *Seismic interpretation: Integrated approach to reservoir characterization*. Schlumberger Oilfield Glossary.

Short, K C. & Stauble, A. J. (1967). *Outline of the geology of Niger Delta*, In Jerry, O. and Efetobore G MO. E. 2021 edition. OI: https://dx.doi.org/10.4314/tjs.v47i5.4.

Stieber S. & Thomas, E. (1975). *The distribution of shale in sandstones and its effect upon porosity*. In SPWLA 16th Annual Logging Symposium, PP 13. Society of Petrophysicists and Well-Log Analysts Yang, Lu, Petrophysical Evaluation of the Trenton-Black River Formation of the Michigan Basin, Master's Thesis, Michigan Technological University in Michele edition 1999. https://doi.org/10.37099/mtu.dc.etds/914.

Telford, W. M., Geldart, L. P., Sheriff, R. E., & Keys, D. A. (1990). *Applied geophysics* (2nd ed.). Cambridge University Press.

Thomas, H., Nsikan, E. & Tejumade, O. (2022). Petrophysical Evaluation of XYZ Field, South-East, Niger Delta Using Well Logs: *International Journal of Earth Sciences Knowledge*

United States Environmental protection Agency (2015). *Assessment of the Potential Impacts of Hydraulic Fracturing for Oil and Gas on Drinking Water Resources. External Review Draft* | EPA/600/R-15/047a. Retrieved from www.epa.gov/hfstudy Office of Research and Development Washington, D.C.

Walid, M. M. & Ziad, B. (2020). Case Study of Petrophysical Evaluation Utilizing Well Logs Data with Optimization of Reservoir Cut-off Parameters, *International Journal of Petroleum Technology*,, 7, pp. 47-49. doi.org/10.15377/2409-787X2020.07.5.

Yergin, D. (1992). In The Epic quest for oil, money and power. a seminar work on energy and policy United States, Jacket design copyright © 1990 pp (57). ISBN D-b71-502Mfl-M.

Yergin, D. (1992). *The prize: The epic quest for oil, money, and power*. Simon & Schuster.

Yilmaz, Ö. (2001). *Seismic data analysis: Processing, inversion, and interpretation of seismic data*. Society of Exploration Geophysicists.

Zhang, D., Sun, M., & Li, J. (2020). Integrating Petrophysical Data for Enhanced Reservoir Characterization: A Case Study. Energy Reports, 6, pp. 1235-1244.

Acknowledgement

I appreciate the almighty God for the grace to achieve this work, my husband Engr. Paschal Chiedozie and daughter Chidera Christabel

Okagu God will bless you for me. I acknowledge the League geoservices limited in partnership with Dhammatan Oil industry limited that gave me the data for this research. I also appreciate Professor Aaron Auduson, Dr. Tope Alege my supervisors, all the members of post graduate board members of the Department of Geology, Federal University lokoja and the entire Postgraduate School Federal University Lokoja, Kogi State for their support.

Compliance with Ethical Standards Declarations

The authors declare that they have no conflict of interest.

Data availability

All data used in this study will be readily available to the public

Availability of data and materials

The publisher has the right to make the data public.

Competing interests

The authors declared no conflict of interest.

Funding

The authors declared no source of funding.

Authors' contributions

This work is part of the first autors master degree thesis and all authors contributed to the wirtting of the manscript, field work and final corrections of the manuscript.